

## Study of the Interaction of Aliphatic Alcohols with TiO<sub>2</sub>

### I. Decomposition of Ethanol, 2-Propanol, and tert-Butanol on Anatase

I. CARRIZOSA AND G. MUNUERA

*Inorganic Chemistry Department, University of Seville, Seville Spain*

Received August 3, 1976; revised February 14, 1977

Adsorption of ethanol, 2-propanol, and tert-butanol has been studied on a well-characterized anatase sample using volumetric and ir techniques. Differences in the adsorption capacities for the three alcohols have been interpreted as due to the same electronic and steric effects that determine changes in the maximum coordination for the Ti<sup>IV</sup> ions in titanium alkoxides. Decomposition of the adsorbed phase was followed by ir and TPD (temperature-programmed decomposition) methods and was compared with the catalytic dehydration of the respective alcohols. The agreement between the kinetic parameters for both processes indicates that the slowest step for the catalytic reaction corresponds to a monomolecular decomposition of the adsorbed species, as supported by studies of water displacement from the anatase surface by all three alcohols.

#### INTRODUCTION

In spite of the considerable attention paid to the study of the adsorption of alcohols on TiO<sub>2</sub> (1-8), little is known about the decomposition of these alcohols catalyzed by TiO<sub>2</sub>, in contrast to the number of papers dealing with this reaction on Al<sub>2</sub>O<sub>3</sub> and SiO<sub>2</sub> (9). Some time ago, Wheeler *et al.* (10) reported gc data on the desorption of ethanol and 2-propanol from metal oxides, including rutile and anatase, from which they concluded that TiO<sub>2</sub> has dehydrogenating activity. This actually contrasts with the more recent results of Jackson and Parfitt (7), who observed that ethyl, *n*-butyl, and *n*-hexyl alkoxides formed during adsorption of the corresponding alcohols on rutile surfaces are thermally decomposed at 300°C, producing surface carbonate species with water and the respective 1-alkene in the gas phase, in agreement with the monomolecular dehydration reported by Knözinger and

Kochloeff (11) for several deuterio-2-propanols on anatase.

In the present paper we have studied the adsorption and decomposition of ethanol (EtOH), 2-propanol (2-PrOH), and tert-butanol (*t*-BuOH) on a well-characterized anatase sample, for which a model of the surface has been previously proposed by us (12). The aim of this work was to obtain further information on the behavior of TiO<sub>2</sub> as a catalyst in the dehydration of such alcohols and, at the same time, to check the use of ir spectroscopy and temperature-programmed decomposition methods in the study of catalytic processes.

#### EXPERIMENTAL

*Materials.* TiO<sub>2</sub> (anatase) had been kindly supplied by British Tioxide (Code No. CL/D 173/2), having been prepared by hydrolysis of titanyl sulfate, followed by heating in air at 700°C. The surface area (25 ± 0.3 m<sup>2</sup> g<sup>-1</sup>) was obtained by the BET

method using  $N_2$  at 77°K. A detailed study of the porosity of this sample has been published elsewhere (13) and has shown that the sample has open V-shaped pores with  $\bar{d} = 28\text{--}29 \text{ \AA}$ .

Conductivity water and EtOH, 2-PrOH, and t-BuOH from Merck (99% purity and redistilled on anhydrous  $CuSO_4$ ) were subjected to several freeze-pump-thaw cycles before use.

*Apparatus and procedures.* Adsorption isotherms up to  $400 \text{ N m}^{-2}$  were determined volumetrically, using 0.7 g of sample in a small-volume system (67 ml) with a silicon oil manometer. Infrared spectra were recorded at room temperature with a Perkin-Elmer 621 double-beam grating spectrometer, using a vacuum cell (14) with a small appendage which could be cooled at 77°K to condense vapors, and a gas sampling device providing gc analysis of the evolved gases.  $TiO_2$  specimens were used in the form of self-supporting disks (40 mg  $cm^{-2}$  and 13 mm $\phi$ ), and a weighed amount of powdered sample was also included, attached to the disk holder to enable simultaneous volumetric adsorption measurements to be made.

Temperature-programmed decomposition (TPD) experiments were carried out in a cell similar to that described by Amenomiya and Cvetanovic (15) using  $N_2$  as carrier gas. A sufficiently high flow rate was selected so that the temperature of the TPD peaks remained flow independent, while the readsorption of products became eliminated. Pulses of the evolved gases were gc analyzed throughout these experiments.

Catalytic activity was measured in a flow system provided with a Pyrex glass reactor. Helium, at a flow rate of 80 ml  $min^{-1}$ , was used as carrier gas under diffusion-free conditions, always using an excess of alcohol in the gas phase to ensure a fully covered surface (pseudo-zero-order reaction). Under such conditions, the reaction rate did not depend on the alcohol pressure, conversions always being lower than 10%. In both TPD

and catalytic experiments, the products were gc analyzed using a Perkin-Elmer F-7 chromatograph with FID detection, provided with a Par-I (Hewlett-Packard) column (2-m length,  $\frac{1}{4}$ -in. diameter).

A treatment of the  $TiO_2$ , consisting of heating in air at 400°C followed by outgassing at 350°C for 4 hr, was used as the standard treatment before adsorption, ir, and TPD experiments, while the same treatment in a He flow (30 ml  $min^{-1}$ ) was used in the catalytic studies after oxidation in air. After such treatment, the surface has characteristic ir and TPD patterns (12), showing only a small number of OH groups ( $\approx 0.3 \text{ OH nm}^{-2}$ ) giving bands at 3730, 3680, and 3620  $cm^{-1}$  and a weak shoulder at 1600  $cm^{-1}$  due to traces of molecular water that were removed only during the TPD scanning at  $t > 450^\circ C$ .

## RESULTS

### *Isotherms and Infrared Spectra*

Figure 1 shows characteristic adsorption isotherms of water and the three alcohols at room temperature on a standard  $TiO_2$  surface. From these isotherms, "irreversible adsorptions" were obtained by subtraction of branch *b* from *a*. In all cases, the "irreversible adsorption" was roughly the value of the adsorption amount at negligible pressure ( $\sim 2.5 \text{ N m}^{-2}$ ), indicating that strong interaction of the adsorbed molecules with the surface occurs. The most noticeable difference between water and the alcohols was the higher capacity of the sample for retaining weakly adsorbed water; this can be related to the possibility of formation of multi-hydrogen-bonded species. Thus, after trapping the gas phase at 77°K, ca. 3  $H_2O \text{ nm}^{-2}$  remained on the surface.

The "irreversible adsorption" for EtOH was slightly higher than that for water, while 2-PrOH and t-BuOH show "irreversible adsorptions" (1.6 and 1.3 molecules  $nm^{-2}$ ), much lower than for EtOH and water.

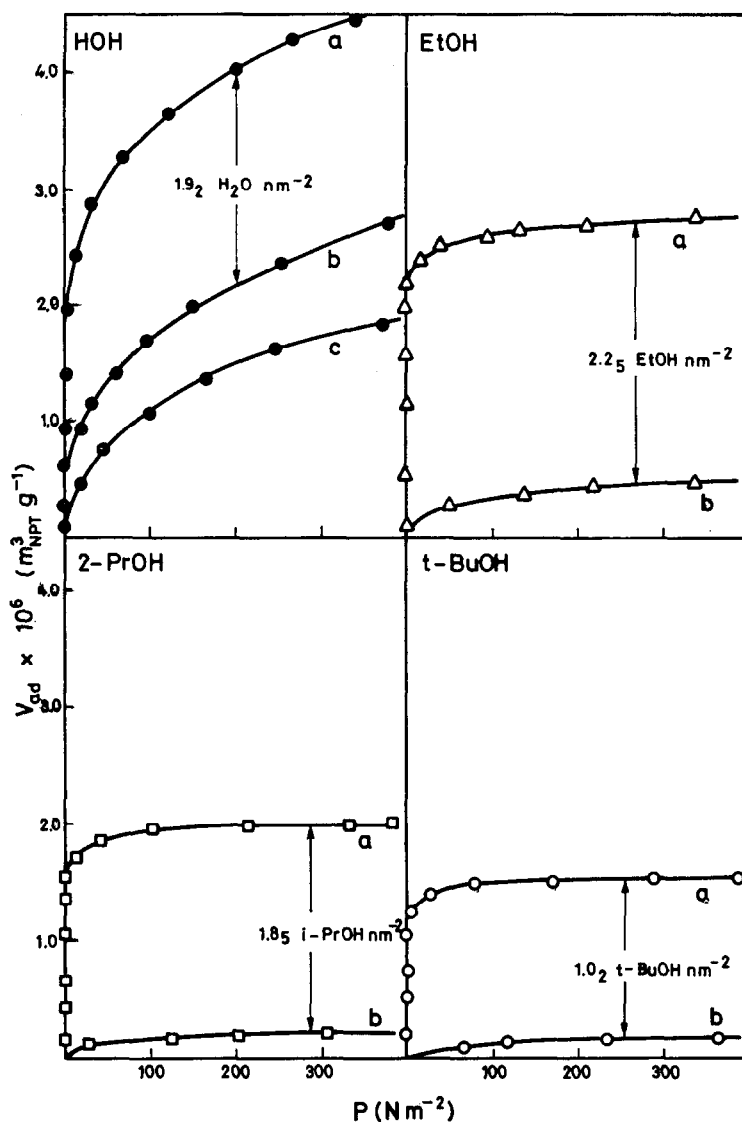


FIG. 1. Adsorption isotherms of water, ethanol, 2-propanol, and tert-butanol on anatase at room temperature. (a) On a standard treated surface; (b) after (a) and evacuation at room temperature for 1 hr; (c) adsorption of water on a sample covered with 2 EtOH nm<sup>-2</sup>.

When the alcohols were adsorbed on the standard surface, two facts were worthy of note and can be seen in Fig. 2. There is, first, the loss of the OH stretch of the unperturbed alcoholic hydroxyl group and, second, the development of a broad band at 3480 cm<sup>-1</sup>, suggesting OH interactions between the adsorbed species and the surface. In order to elucidate the type of interactions involved in the alcohol adsorption,

and until reaching the "irreversible adsorption" coverages, small doses were adsorbed at room temperature on the standard treated surface, and infrared spectra were recorded in the usual way, as shown in Fig. 3 for EtOH. By plotting the absorbances of  $\nu_{\text{OH}}$  and  $\nu^{\text{asym}}_{\text{CH}_3}$  stretching bands against the coverage (Fig. 4), several features for the three alcohols could be observed. For all alcohols, the absorbances of both the broad

band at  $3480\text{ cm}^{-1}$  and the  $\nu^{\text{asym}}\text{CH}_3$  band increase linearly with the alcohol coverages, fulfilling Beer's Law, until a "critical coverage" is reached. As shown in Fig. 4, this "break point" for EtOH was at a coverage of ca. 2 molecules  $\text{nm}^{-2}$ , while, in the case of 2-PrOH and t-BuOH, it was at ca. 1 molecule  $\text{nm}^{-2}$ . Similar behavior was observed for the surface OH band at  $3730\text{ cm}^{-1}$  that, in this case, decreased slowly with a

constant slope up to the "break point" and, thereafter, more sharply.

In spite of the difficulty of determining these actual absorbances with accuracy, the two small bands at  $3680$  and  $3620\text{ cm}^{-1}$  follow a rather similar pattern, first increasing up to the "break point" and then decreasing. However, the relative changes of these two bands were different from primary, secondary, and tertiary alcohols,

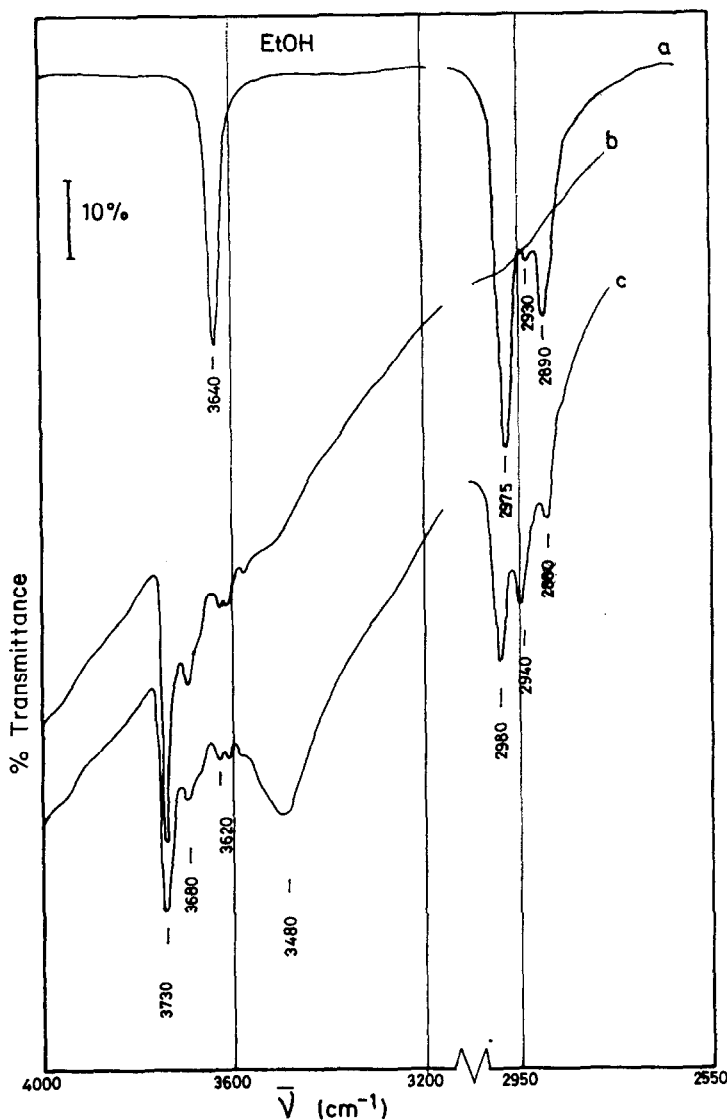


FIG. 2. Infrared spectra of: (a) EtOH diluted in  $\text{CCl}_4$ ; (b) anatase standard surface; (c) EtOH adsorbed on anatase (coverage,  $0.80\text{ EtOH nm}^{-2}$ ).

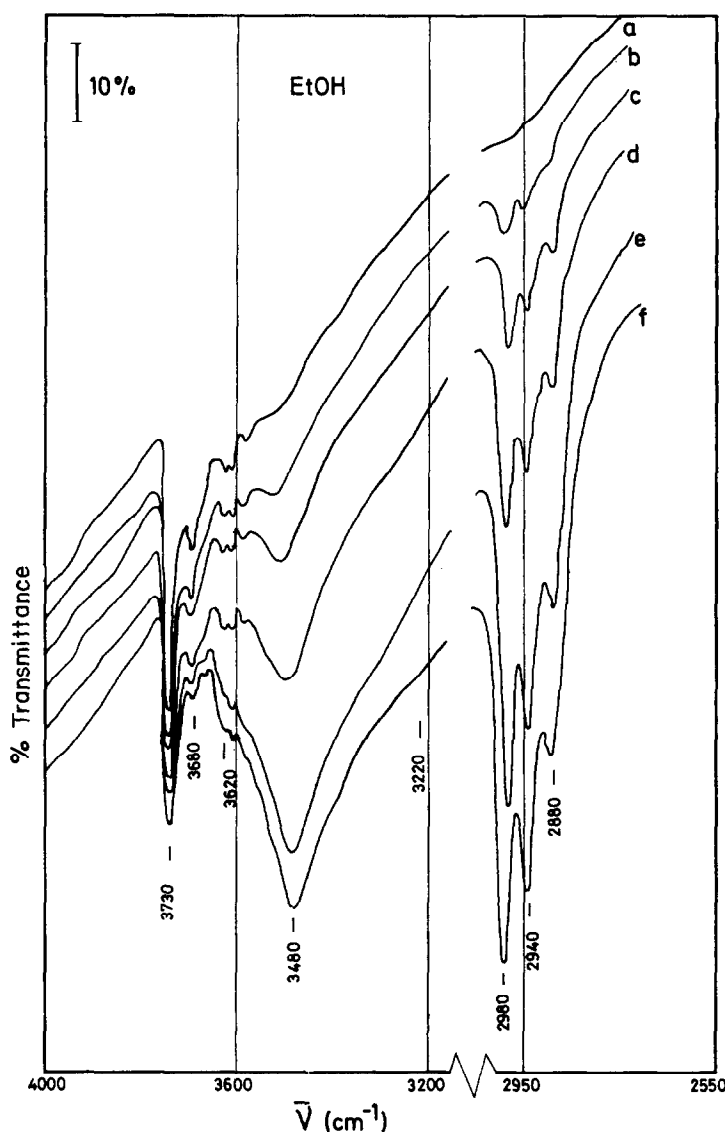


FIG. 3. Infrared spectra of ethanol adsorbed on anatase (coverages in EtOH  $\text{nm}^{-2}$ ): (a) standard surface; (b) 0.49; (c) 1.07; (d) 1.76; (e) 2.30; (f) 2.58.

as can be seen in Fig. 4. The behavior of the OH bands during adsorption of doses of water is shown for comparative purposes. It can be seen that bands at 3680 and 3620  $\text{cm}^{-1}$  sharply increase for coverages higher than 1  $\text{H}_2\text{O nm}^{-2}$ , though the band at 3730  $\text{cm}^{-1}$  remains at the same intensity up to coverages of 2  $\text{H}_2\text{O nm}^{-2}$ .

#### *Decomposition of the Adsorbed Phase*

Decomposition of the adsorbed alcohols was studied by the TPD technique, using

several heating rates in order to evaluate the kinetic parameters. Characteristic TPD traces for water and the three alcohols are shown in Fig. 5. Analysis of pulses of the evolved gases during TPD scanning (shown only for ethanol in this figure) indicates that all three alcohols decompose, giving olefins and water as the main products. In the case of EtOH, the first broad TPD peak at 250°C corresponds to desorption of the alcohol. A simple calculation from

the flow rate of the carrier gas and the gc calibration indicated that the recovered alcohol was about 50% of the total coverage; thus, only ca. 1 EtOH nm<sup>-2</sup> should decompose during TPD scanning. The sharper TPD peak at 340°C was due to ethylene and water, as shown by the gc analysis of the pulses. However, butenes and diethyl ether were also detected in this range of temperatures, though the amounts of these products were always lower than 5% of the evolved olefin at each particular temperature. In the cases of 2-PrOH and t-BuOH, the TPD traces in Fig. 5 indicate that a small amount of alcohol was also desorbed, unreacted as confirmed by gc analysis (not shown in the figure), leaving coverages of ca. 1 ROH nm<sup>-2</sup>.

In connection with these alcohols, it is noteworthy that, in the case of t-BuOH, the olefin isobutene evolves at 180°C, a temperature considerably lower than that for water desorption, which gives the peak at 250°C in the same TPD trace. For 2-PrOH, water and propylene evolve at almost the same temperature, giving a single peak at ca. 280°C.

Using different heating rates ( $\beta$  between 4 and 30°C min<sup>-1</sup>) and assuming a first-order reaction for the olefin formation, the kinetic parameters for the decomposition of the three alcohols were obtained from the temperatures of the TPD peaks ( $T_M$ ) due to olefin evolution, by using the

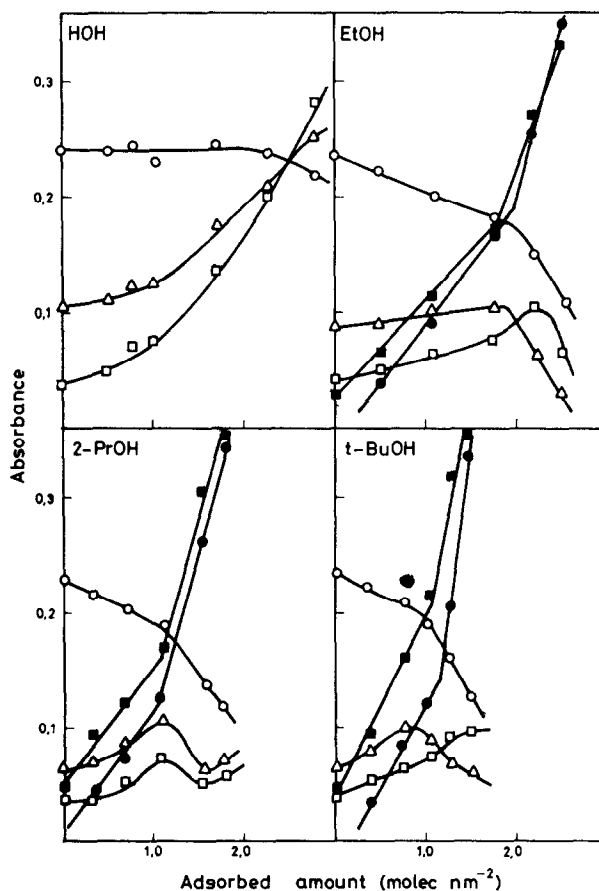


FIG. 4. Changes of absorbance for the  $\nu_{OH}$  of the free surface OH groups and the  $\nu_{asym}^{CH_3}$  against adsorption coverages of alcohols. (○) 3730; (△) 3680; (□) 3260; (●) 2975; (■) 3480 cm<sup>-1</sup>.

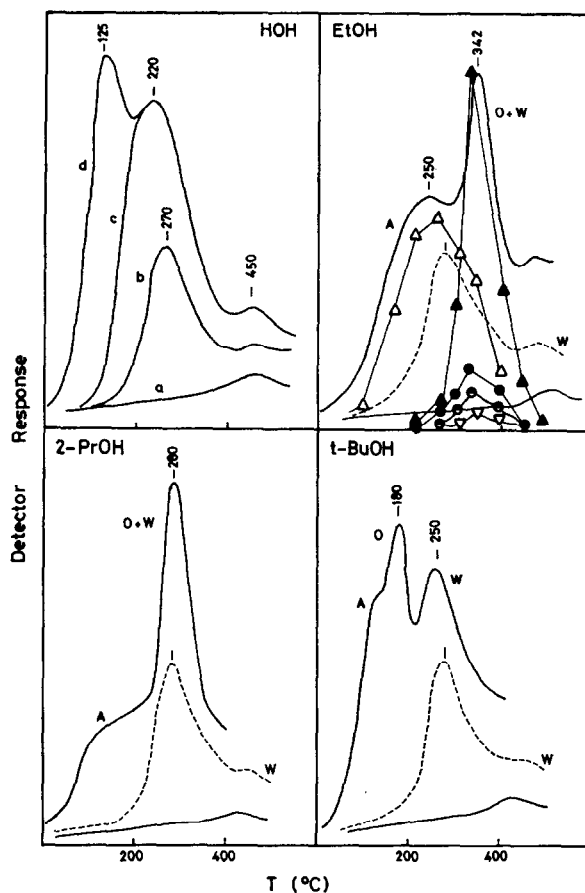


FIG. 5. TPD traces of water and alcohols adsorbed on anatase ( $\beta = 16^\circ\text{C min}^{-1}$ ). Water: (a) standard surface; (b) covered with  $1 \text{ H}_2\text{O nm}^{-2}$ ; (c) covered with  $2 \text{ H}_2\text{O nm}^{-2}$ ; (d) covered with  $3 \text{ H}_2\text{O nm}^{-2}$ . Alcohols: in all cases, the dashed line corresponds to the TPD trace of  $1 \text{ H}_2\text{O nm}^{-2}$ , and the TPD trace of the standard sample is included. A, Alcohol; O, olefin; W, water. Analyses of pulses for ethanol: ( $\Delta$ ) ethanol; ( $\nabla$ ) diethyl ether; ( $\blacktriangle$ ) ethylene; ( $\bullet$ ) 1-butene; ( $\ominus$ ) *trans*-2-butene.

equation:

$$2 \log T_M - \log \beta = E/2.3RT_M + \log (E/AR),$$

$E$  being the activation energy and  $A$  the frequency factor. The calculated values for  $E$  and  $A$  are given in Table 1, together with the kinetic parameters for the desorption of water with an initial coverage of  $1 \text{ H}_2\text{O nm}^{-2}$  from the standard surface (16). This latter value was somewhat higher than the  $32 \text{ kJ mol}^{-1}$  obtained for the desorption of water formed during TPD experiments with *t*-butanol.

Data in Table 1 show that values of  $A$  (in seconds) $^{-1}$  are rather low for all three alcohols, though of the same order as those reported by other authors (17) for this type of reaction on metal oxides.

In order to check the credibility gap of the above values and their independence of the experimental technique (TPD method), a set of experiments was carried out to determine the kinetic parameters from the thermal evolution of  $\nu_{\text{CH}}$  bands in the ir spectra of the adsorbed species. In these experiments, EtOH, 2-PrOH, and *t*-BuOH were adsorbed on a standard

TABLE 1

TPD Kinetic Parameters for Alcohol Dehydration and Water Desorption from an Anatase Surface

Preadsorbed species	Activation energy (kJ mol <sup>-1</sup> )	Frequency factor (s <sup>-1</sup> )
EtOH	76.5 ± 2	1.4 × 10 <sup>4</sup>
2-PrOH	92.4 ± 2	4.7 × 10 <sup>6</sup>
t-BuOH	53.9 ± 2	9.8 × 10 <sup>3</sup>
Water	50-54	1.0 × 10 <sup>3</sup>

TABLE 2

Infrared Kinetic Parameters for Alcohol Dehydration on an Anatase Surface

Preadsorbed species	Activation energy (kJ mol <sup>-1</sup> )	Frequency factor (s <sup>-1</sup> )
EtOH	78.6 ± 5	1.0 × 10 <sup>4</sup>
2-PrOH	92.8 ± 5	4.8 × 10 <sup>6</sup>
t-BuOH	56.0 ± 5	2.0 × 10 <sup>4</sup>

surface and were decomposed at several temperatures, while the reaction was monitored by recording changes of the  $\nu^{\text{asym}}_{\text{CH}}$  band at 2980–2975 cm<sup>-1</sup>. Initial coverages were in all cases kept lower than 1 molecule nm<sup>-2</sup>, thus allowing only a single species to exist on the surface, so that Beer's Law can be applied. In these experiments the TiO<sub>2</sub> disk was moved, for a measured short time, into the furnace of the ir cell, previously stabilized at a preset temperature, and was then quenched at room temperature, and the absorbance of the  $\nu_{\text{CH}}$  band was recorded. During the experiment, the evolved gases were trapped at 77°K and then were gc analyzed at the end of the

experiment, thus confirming that the main products were olefins. However, small traces of butenes and diethyl ether were detected when using EtOH, as previously observed during the TPD experiments.

After heating at 400°C for 1 hr, the ir spectrum of the original surface was restored, showing its hydroxyl bands at 3730, 3680, and 3620 cm<sup>-1</sup> with their original intensities.

Straight lines were obtained when values of log  $A$  ( $A$  is absorbance of the  $\nu^{\text{asym}}_{\text{CH}}$  band) were plotted against the total time of heating at each particular temperature, thus confirming the first-order reaction in all cases. The rate constant values ob-

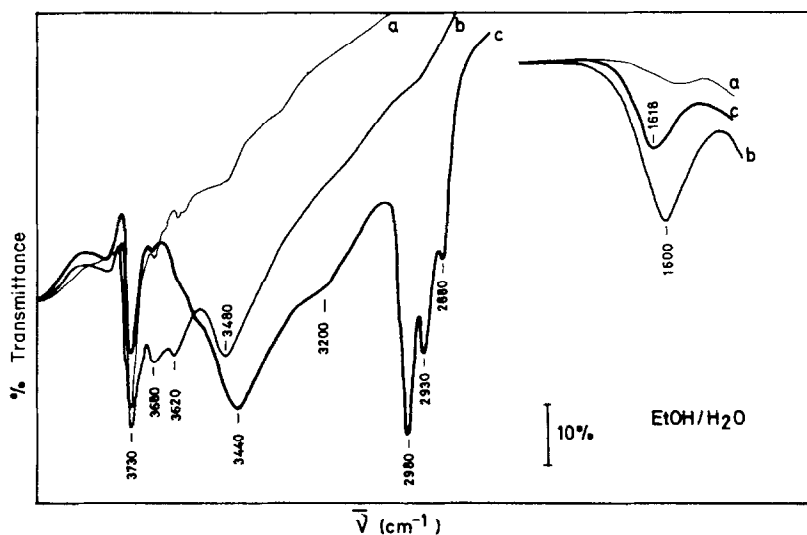


FIG. 6. Infrared spectra for the water displacement experiment: (a) standard surface; (b) covered with 1.80 H<sub>2</sub>O nm<sup>-2</sup>; (c) after equilibration with excess of ethanol.



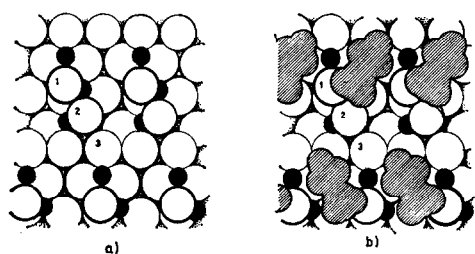


FIG. 7. (a) Plane view of the (111) stoichiometric cleavage plane of anatase (12). (b) Adsorption model for ethanol adsorbed on this plane.

tained from these lines fulfill the Arrhenius equation, from which kinetic parameters were calculated (data compiled in Table 2). The values agree fairly well with those previously obtained by TPD method, thereby corroborating the first-order reaction assumed in the TPD calculations. Furthermore, as experiments were carried out under vacuum, diffusion control on the reaction rate can be eliminated.

#### Displacement of Water by Alcohols

In order to check the possible influence of the decomposition products, particularly water, the desorption of which has been proposed as the controlling step in catalytic dehydration of alcohols by Krylov (18), volumetric and ir displacement studies were carried out at room temperature using a standard surface previously covered with ca.  $1.8 \text{ H}_2\text{O nm}^{-2}$ ; after recording the ir spectrum, a measured amount of alcohol exceeding the adsorption capacity of the

TABLE 3

Adsorbed Species on Anatase Surface after Partial Displacement of Water by Alcohols at Room Temperature

Alcohol	Adsorbed alcohol (molecules $\text{nm}^{-2}$ )	Adsorbed water (molecules $\text{nm}^{-2}$ )
EtOH	2.00	1.00
2-PrOH	1.60	1.40
t-BuOH	1.30	1.40

TABLE 4

Catalytic Flow Reactor Kinetic Parameters of Alcohol Dehydration on an Anatase Surface

Alcohol	Activation energy ( $\text{kJ mol}^{-1}$ )	Frequency factor (molecules $\text{m}^{-2} \text{ s}^{-1}$ )
EtOH	$79.4 \pm 2$	$1.1 \times 10^{22}$
2-PrOH	$91.5 \pm 2$	$1.4 \times 10^{26}$
t-BuOH	$56.4 \pm 2$	$1.4 \times 10^{23}$

sample was admitted at room temperature and was placed in contact with the hydrated surface, until no changes of pressure were observed. The gas phase and the weakly adsorbed species were condensed at  $77^\circ\text{K}$ , and the ir spectrum was recorded again. Meanwhile, the total amount of condensed vapors (water plus alcohol) was measured volumetrically. Figure 6 shows the ir spectra of the anatase surface during these experiments with EtOH, while similar patterns were obtained for the other two alcohols. The amount of alcohol adsorbed in these experiments was evaluated from the absorbances of the  $\nu_{\text{CH}}$  band, with the aid of the absorbance/coverage plots in Fig. 4, while the amount of water remaining at the surface was calculated by subtracting the quantity of nonadsorbed alcohol from the total amount of the condensed vapors. Data obtained in this way for all three alcohols have been summarized in Table 3.

As shown in Fig. 6, adsorption of the alcohols on a water-covered surface disturbs the ir spectrum of the adsorbed water. For all three alcohols, the intensity of the bands at  $3680$  and  $3620 \text{ cm}^{-1}$  noticeably decreases, while the broad band at  $3480 \text{ cm}^{-1}$  broadens and moves to  $3440 \text{ cm}^{-1}$  with a shoulder at  $3200 \text{ cm}^{-1}$ , the sharp bands of  $\nu_{\text{CH}}$  now appearing in the spectra. In the bending region of water, the intensity of the original band at  $1600 \text{ cm}^{-1}$  decreases in the order  $\text{EtOH} > 2\text{-PrOH} > \text{t-BuOH}$ , while it becomes asymmetric and displaced

toward higher wavenumbers (1618, 1613, and 1608  $\text{cm}^{-1}$  for EtOH, 2-PrOH and *t*-BuOH, respectively). These two facts confirm that alcohols displace water from their adsorption centers, though the extension of this displacement depends on the alcohol itself.

#### *Catalytic Dehydration of the Alcohols*

Catalytic decomposition of the three alcohols under pseudo-zero-order conditions (fully covered surface) gave olefin and water exclusively, except for EtOH, where traces of butenes and ether could be detected again, though always in a percentage lower than 3% of the olefin. Arrhenius plots for all three alcohols gave the kinetic parameters compiled in Table 4.

By comparing the activation energy for the catalytic dehydration with those activation energies previously obtained for the thermal decomposition of the adsorbed phase from TPD or ir data, good agreement was observed. This agreement suggests that, under the above conditions, the catalytic process involves the adsorbed species that must decompose in a manner very similar to that in the TPD or ir experiments, suggesting that the role of alcohol in the gas phase during the catalytic process was only to dislodge the water molecules produced during the reaction from their adsorption sites and, thus, close the catalytic cycle.

### DISCUSSION

#### *Adsorption*

The adsorption capacity of the anatase surface pretreated under the standard conditions used in this work [almost completely dehydroxylated (16)] depends on the type of alcohol, decreasing with the length of the hydrocarbon chain. The values for "irreversible adsorption" are rather low for all three alcohols, as can be shown by calculation of the cross section of each alcohol from its density in the

liquid state (14), and, therefore, the adsorbed molecules should be rather sparsely distributed over the surface, so we may conclude that specific interactions occur between the alcohol molecules and surface sites.

In the case of EtOH, the "irreversible adsorption" was 2.25 EtOH  $\text{nm}^{-2}$ , not far from the value reported for water (12), which suggests that the same type of centers should be involved in the adsorption of both species. However, infrared spectroscopy was found to be more sensitive for discriminating between different types of adsorptions. Thus, Fig. 4 clearly suggests that, for EtOH and water, adsorption occurs in the same way, only up to a coverage of ca. 2 molecules  $\text{nm}^{-2}$ , while, for higher coverages, new forms of adsorption appear. The amount of more tightly adsorbed ethanol, 2 EtOH  $\text{nm}^{-2}$ , agrees with the number of more exposed  $\text{Ti}^{\text{IV}}$  ions on the anatase surface (1.9  $\text{Ti}^{\text{IV}}$   $\text{nm}^{-2}$ ), as calculated from the surface model shown in Fig. 7a and previously proposed for this oxide (12). This fact clearly suggests that adsorption must take place with the ethanol acting as a bridging ligand between two neighboring  $\text{Ti}^{\text{IV}}$  ions, filling the coordinative unsaturation of these ions, as shown in Fig. 7b. However, TPD experiments illustrated in Fig. 5 indicate that ca. 50% of this adsorbed ethanol is easily removed from the surface without decomposition, indicating that half of the adsorbed molecules should be more weakly bonded than the remaining 1 EtOH  $\text{nm}^{-2}$  that decomposes upon heating to give mainly olefin. This seems to suggest that the sixfold coordination attained by the  $\text{Ti}^{\text{IV}}$  ions at the surface with two bridging alcohol molecules, as shown in Fig. 7b, is rather unstable, and desorption of 1 EtOH  $\text{nm}^{-2}$  occurs giving a surface with  $\text{Ti}^{\text{IV}}$  ions in an average fivefold coordination, resulting from alternate elimination of the alcohol molecules (Fig. 7b). Similar behavior had been reported previously by us (16) for

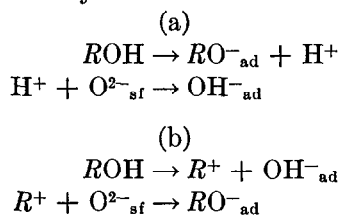
the desorption of 50% of the "irreversible adsorbed" water from this anatase sample.

According to the above conclusion, the tight adsorption for 2-PrOH and *t*-BuOH corresponds to ca. 1 molecule nm<sup>-2</sup>, the same as for ethanol, but, with these two alcohols, the maximum coordination number (6) for the surface Ti<sup>IV</sup> ions could not be completely attained by saturation with alcohol vapor (only 1.6 and 1.3 molecules nm<sup>-2</sup>, respectively). The situation seems to be rather similar to that existing in titanium alcoholates, Ti(OR)<sub>4</sub>, in which differences in coordination from 6 to 4 occur with increasing complexity of the alkyl group, so that Ti(OMe)<sub>4</sub> and Ti(OEt)<sub>4</sub> have hexacoordinated Ti<sup>IV</sup> ions with bridging alkoxide groups, while Ti(O *t*-Bu)<sub>4</sub> is a monomeric liquid in which the Ti<sup>IV</sup> ions have a fourfold coordination (19). Therefore, adsorption of alcohols up to 1 ROH nm<sup>-2</sup> leads to a half-covered surface in which each Ti<sup>IV</sup>, originally in a fourfold coordination, will accept a fifth bridging ligand at alternated Ti<sup>IV</sup> pairs. A further adsorption on this surface must accomplish the sixfold coordination of the cations, but inductive as well as steric effects of the highly nucleophilic and bulky ligands may limit this second state for 2-PrOH and *t*-BuOH but not for EtOH or water.

Provided that the total number of molecules, even in the case of EtOH, is rather small compared with the density of the liquid alcohol or the respective alcoholates, we may conclude that electronic saturation should be the more important factor in determining the coordination number after saturative adsorption, now that, as shown in Fig. 7b, all three alcohols can be easily packed on the surface, thus discarding steric effects. In summary, the increasing donor capacity of the alcohol molecules with the size and branching of the alkyl group may lead to a saturation of the Ti<sup>IV</sup> charge that produces a leveling off of the adsorption capacity in agreement with the

well-known electroneutrality principle of Pauling.

The broad band at 3480 cm<sup>-1</sup> suggests that the coordinative adsorption occurs mainly in a nondissociative way, the hydrogen of the alcohol group being involved in H bonding to neighboring O<sup>2-</sup> ions at the surface, as previously proposed by Jackson and Parfitt (7). In addition to the main nondissociative adsorption of the alcohols, two possibilities exist for the small dissociative adsorption that occurs simultaneously:

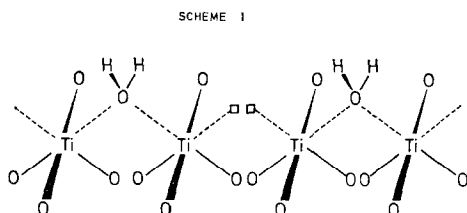


where (ad = adsorbed and sf = surface).

Form (a) should be more likely for EtOH and leads to the rise of the band at 3620 cm<sup>-1</sup> that, according to our previous model for the surface, corresponds to residual OH groups in some of the positions labeled 3 in Fig. 7a. Mechanism (b) should increase in importance for 2-PrOH and *t*-BuOH due to the inductive effect of their alkyl chains. The new OH groups should be packed between oxygen atoms labeled 2 in that figure, outside the coordination sphere of the more exposed Ti<sup>IV</sup> ions, giving rise to the band at 3680 cm<sup>-1</sup>. Highly nucleophilic oxygens, labeled 1, may now participate in the second step of alcoholate formation through mechanism (b); this leads to a fourfold coordination of some of the surface Ti<sup>IV</sup> ions, even after adsorption of the alcohols. This may also contribute to the more rapid decrease of the 3730 cm<sup>-1</sup> OH band in the cases of 2-PrOH and *t*-BuOH adsorption, due to highly basic OH groups in some of the positions labeled 1 in Fig. 7a.

A further comparison can be made between the changes observed in the intensities of the OH stretching bands with increasing coverages of water and those

observed in the case of the alcohols (Fig. 4). Previous studies (12) suggest that adsorption of water should occur at an early stage as a bridging ligand filling half of the coordination positions of the fourfold-coordinated  $Ti^{IV}$  ions at the surface, according to:



This water gives a TPD peak at  $270^{\circ}C$  and a broad ir band centered at  $3480\text{ cm}^{-1}$ , as shown in Figs. 4 and 7, respectively. Further adsorption up to  $2\text{ H}_2\text{O nm}^{-2}$  displaces the TPD peak to  $220^{\circ}C$ , and, together with the band at  $3480\text{ cm}^{-1}$ , bands at  $3620$  and  $3680\text{ cm}^{-1}$  appear with the same wavenumber as the isolated OH groups remaining on the outgassed anatase surfaces. Higher coverages lead to a new type of adsorption characterized by a TPD peak at  $125^{\circ}C$  (Fig. 5), together with a displacement of the bending mode of the water from  $1600$  to  $1610\text{ cm}^{-1}$ , which has been explained (12) by assuming that, under these conditions, the adsorbed molecules are subjected to an asymmetric field, probably involving some hydrogen bonding with a mainly electrostatic interaction.

As can be observed in Fig. 6, the bands at  $3680$  and  $3620\text{ cm}^{-1}$  in the water-covered sample are immediately removed after adsorption of alcohol, suggesting that this water is easily displaced by the alcohol molecules from the gas phase. Volumetric and ir data confirm this fact, though some water remains on the surface, which gives with the alcohol a total coverage of  $2.7\text{--}3.0$  molecules  $\text{nm}^{-2}$ . This residual nondisplaced water gives a very asymmetric bending mode displaced toward higher wavenumbers, the shift of the band depending upon

the alcohol. A comparison of the fully hydrated anatase surface holding ca.  $3\text{ H}_2\text{O nm}^{-2}$  and the surface resulting from the displacement of water by ethanol ( $2\text{ EtOH nm}^{-2}$  plus  $1\text{ H}_2\text{O nm}^{-2}$ ) shows that an important difference between the ir spectra of both surfaces occurs in the  $1600\text{-cm}^{-1}$  region. While in the hydrated surface the third water molecule only slightly displaces its bending mode from  $1600$  to  $1610\text{ cm}^{-1}$ , in the case of adsorbed ethanol this band is asymmetric and appears at  $1618\text{ cm}^{-1}$ , suggesting a situation different from that of the water remaining in this surface. Indeed, the low reversible adsorption of water on a surface holding  $2\text{ EtOH nm}^{-2}$  (Fig. 1, isotherm c of HOH) suggests that EtOH does not completely displace water, which partially remains at the coordination sphere of the  $Ti^{IV}$  ions. Therefore, during displacement experiments, EtOH molecules in the gas phase must attack the bridging water ligands, producing almost complete displacement of these molecules from the coordination sphere of the surface  $Ti^{IV}$  ions; a small amount of this water can remain on the coordination positions of the cations, together with the alcohol, giving rise to the band at  $1618\text{ cm}^{-1}$ , characteristic of a high electron density on these water molecules held by fully coordinated  $Ti^{IV}$  ions. It should be emphasized that the existence of bridging ligands and/or free coordination positions around the cations should be of paramount importance in facilitating and promoting the nucleophilic attack of the alcohol molecules.

In the cases of 2-PrOH and t-BuOH, the situation seems to be somewhat different. Only  $1.6$  and  $1.3$  molecules  $\text{nm}^{-2}$  of these alcohols are retained on the water-covered surface, the same values as for the ir "irreversible adsorptions" on a standard sample, while some water remains adsorbed, completing a  $2.7\text{--}3.0$  molecules  $\text{nm}^{-2}$  coverage. Then, 2-PrOH and t-BuOH can be adsorbed by opening alternating

water bridging ligands on the coordination sphere of the  $Ti^{IV}$  and displacing half of the water molecules, as with EtOH. However, when alcohol adsorbs according to scheme (b), the coordination number around the exposed  $Ti^{IV}$  should not increase, and the water molecules will remain on the surface, generally in their original positions. Whatever the situation, it can be expected that the bending mode of water does not become displaced too far from its original position at  $1600\text{ cm}^{-1}$ , as actually observed for these two alcohols.

### *Decomposition*

The first point to be emphasized is the absence of ethers as decomposition products; traces of diethyl ether were observed only in the case of ethanol, in the same range of temperature as observed in TPD evolution of ethylene. This fact suggests that, on anatase, monomolecular dehydration of the alcohols is produced more easily than is the dimolecular process. This behavior is rather different from that observed by Knözinger (20) in the case of alumina catalysts, where formation of ethers has been related to the existence of well-defined alcoholate species upon adsorption of normal aliphatic alcohols. On the other hand, traces of butenes were also detected together with ethylene in all decomposition experiments with EtOH, suggesting a Ziegler-Natta oligomerization process, probably involving alkyl-titanium species formed on the surface during decomposition of alcohol, as will be discussed in a forthcoming paper.

According to the reaction stoichiometry,

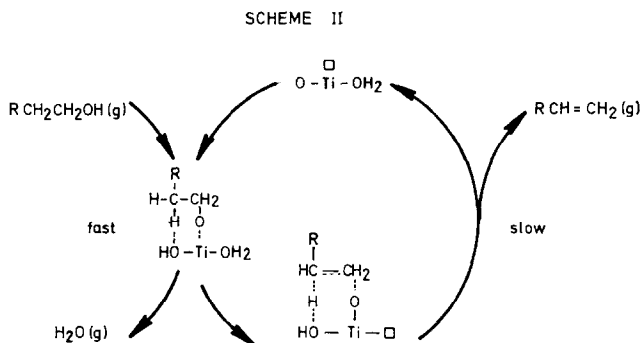


about  $1\text{ H}_2\text{O nm}^{-2}$  should be produced in TPD experiments with all three alcohols.

This water should give a TPD peak at  $270^\circ\text{C}$  in the case of a free standard surface (shown by dashed lines in Fig. 5); this temperature is lower than that for decomposition of EtOH itself. Therefore, upon decomposition of this alcohol in the range  $300\text{--}350^\circ\text{C}$ , water must be immediately desorbed from the surface. For 2-PrOH, the decomposition temperature coincides with that for desorption of  $1\text{ H}_2\text{O nm}^{-2}$  from a standard surface, indicating that both alcohol decomposition and desorption of the water formed in the reaction must occur simultaneously. However, in the case of t-BuOH, the olefin isobutene emerges early in the TPD scanning, giving a peak at  $180^\circ\text{C}$ , followed by the water in a well-differentiated peak at  $250^\circ\text{C}$ , a temperature that is slightly lower than that for desorption of  $1\text{ H}_2\text{O nm}^{-2}$  from the standard surface. It is noteworthy that the activation energy for water desorption ( $33\text{ kJ mol}^{-1}$ ) was lower here than for the evolution of the olefin. Thus, the high temperature of water evolution must be ascribed to an entropy effect rather than to enthalpy differences. Desorption would require an important loss of entropy of the adsorbed water molecules that should be considered as forming a mobile phase on the surface, under the decomposition conditions.

If no other factors influence the rate of decomposition, desorption of water from the active centers should be the controlling step, at least in the dehydration of t-BuOH. However, displacement experiments illustrate very clearly the importance of the dislodging capacity of the alcohol molecules from the gas phase in removing from the surface the water molecules produced during the reaction. By comparing Fig. 5 with the ir spectra in Fig. 6 we may conclude that the nucleophilic attack of the alcohol molecules in the gas phase on the  $Ti^{IV}$  which holds the adsorbed water is of paramount importance in deciding the con-

trolling step of the catalytic cycle:



The existence of vacancies in the coordination sphere of these  $\text{Ti}^{\text{IV}}$  ions plays an important role in this displacement process. Thus, if the nucleophilicity of the *t*-BuOH molecules weakens the strength of the bond of the adsorbed water, making the displacement easier than the decomposition of the alcohol itself, the whole process will also be controlled here by the surface reaction step in the presence of this alcohol in the gas phase. Indeed, this latter condition might not be required in the cases of 2-PrOH and EtOH, since water desorption and alcohol decomposition occur at the same temperature and, so, the produced water should immediately leave the surface.

The results for catalytic dehydration of the three alcohols, in fair agreement with those for TPD decomposition of the adsorbed phase, support the above conclusion. Moreover, the ir spectra indicate that, after decomposition of the adsorbed phase, the surface completely recovers its original state, thus allowing a new catalytic cycle. This is actually the only condition required for TPD kinetic data to be comparative with those directly obtained under catalytic steady-state conditions. Contrary to Knözinger's view (9), in the above circumstances, the study of the decomposition of the adsorbed phase really may provide conclusions on the catalytic dehydration mechanism, and kinetic parameters for the

catalytic reaction can be drawn from the thermal decomposition studies of the adsorbed phase.

By dividing the values of the rate constants in Table 4 by the preexponential factors of the Arrhenius equation in Table 1 or 2, the number of active sites under catalytic conditions can be estimated as  $10^{14}$ – $10^{15}$   $\text{cm}^{-2}$ . This seems reasonable under the experimental conditions used in the flow reactor, with a pressure of alcohol on the catalyst giving a fully covered surface (pseudo-zero order). This leads to the conclusion that the low values for the frequency factors given in Table 1, compared with those predicted by transition-state theory should be ascribed to an entropy effect. A simple calculation (21) indicates that the decrease of ca. 30 e.u. observed with these alcohols may be due to the loss of the translational and rotational freedom of the adsorbed molecules on the surface when they form the transition state leading to the reaction products, thus suggesting a transition state with a two-point interaction as in an  $E_2$  mechanism.

#### REFERENCES

1. Shchekochikhin, Y. M., Filimonov, V. N., Keyer, N. P., and Terenin, A. N., *Kinet. Katal.* **5**, 113 (1964).
2. Kiselev, A. V., and Uvarov, A. V., *Surface Sci.* **6**, 399 (1967).

3. Knözinger, H., *Z. Phys. Chem.* **69**, 108 (1970).
4. Day, R. E., and Parfitt, G. D., *Powder Technol.* **1**, 3 (1967).
5. Day, R. E., and Parfitt, G. D., *Trans. Faraday Soc.* **64**, 815 (1968).
6. Day, R. E., Parfitt, G. D., and Peacock, J., *Discuss. Faraday Soc.* **52**, 215 (1971).
7. Jackson, P., and Parfitt, G. D., *J. Chem. Soc. Faraday Trans. 1* **68**, 1443 (1972).
8. Munuera, G., and Stone, F. S., *Discuss. Faraday Soc.* **52**, 205 (1971).
9. Knözinger, H., in "The Chemistry of the Hydroxyl Group," (S. Patai, Ed.), p. 641. Interscience, New York, 1971, and references therein.
10. Wheeler, D. J., Darby, P. W., and Kembal, C., *J. Chem. Soc.* 332 (1960).
11. Knözinger, H., and Kochloeff, K., in "Proceedings, 5th International Congress on Catalysis" (J. W. Hightower, Ed.), Vol. 2, p. 1171. North-Holland, New York, 1973.
12. Munuera, G., Moreno, F., and Gonzalez, F., in "Proceedings, 7th International Symposium on Reactivity of Solids" (J. S. Anderson, M. W. Roberts, and F. S. Stone, Eds.), p. 681. Chapman and Hall, London, 1972.
13. Munuera, G., Carrasco, J., and Gonzalez, F., *Anal. Fis. Quim.* **67B**, 516 (1971).
14. Carrizosa, I., Ph.D. thesis. University of Seville, Seville, 1973.
15. Amenomiya, Y., and Cvetanovic, R. J., in "Advances in Catalysis" (D. D. Eley, H. Pines, and P. B. Weisz, Ed.), Vol. 17, p. 103. Academic Press, New York, 1967.
16. Carrizosa, I., Moreno, F., and Munuera, G., *Anal. Fis. Quim.* **67B**, 919 (1971).
17. Knözinger, H., Buhl, H., and Kochloeff, K., *J. Catal.* **24**, 57 (1970).
18. Krylov, O. V., *Zh. Fiz. Khim.* **39**, 2656 (1965).
19. Bradley, D. C., in "Progress in Inorganic Chemistry" (F. A. Cotton, Ed.), Vol. 2, p. 303. Interscience, New York, 1960.
20. Knözinger, H., *Angew. Chem. Int. Ed. Engl.* **7**, 791 (1968).
21. Kembal, C., in "Advances in Catalysis" (W. G. Frankenburg, V. I. Komarewsky, and E. K. Rideal, Eds.), Vol. 2, p. 233. Academic Press, New York, 1950.